Inorganic Chemistry

Article

pubs.acs.org/IC

# Synthesis and Study of Three Novel Macrocyclic Selena[*n*]ferrocenophanes Containing a Naphthalene Unit

Wei Ji,[†,∥] Su Jing,*[,†,‡] Zeyu Liu,[§] Jing Shen,[†] Jing Ma,*[,§] Dunru Zhu,*[,∥] Dengke Cao,[‡] Limin Zheng,[‡] and Minxia Yao[†]

[†]College of Sciences, Nanjing University of Technology, Nanjing 211816, China

[‡]State Key Laboratory of Coordination Chemistry, Nanjing University, Nanjing 210008, China

[§]Institute of Theoretical and Computational Chemistry, School of Chemistry and Chemical Engineering, Nanjing University, Nanjing 210093, China

[∥]College of Chemistry and Chemical Engineering, State Key Laboratory of Materials-oriented Chemical Engineering, Nanjing University of Technology, Nanjing 210009, China

Supporting Information

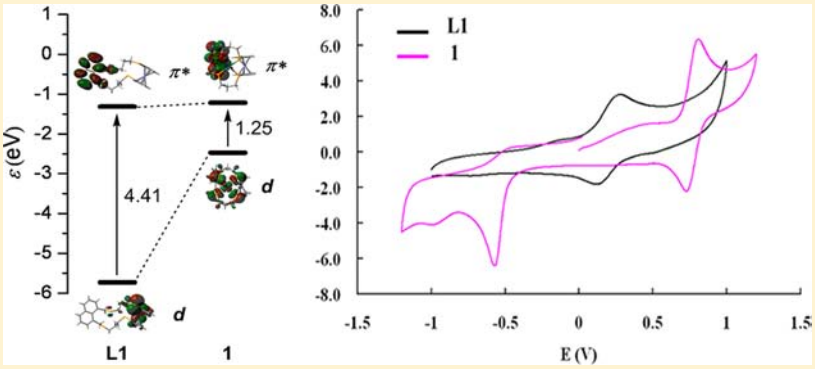


**ABSTRACT:** Three novel macrocyclic ligands, **L1**−**L3**, in which a ferrocene unit and a fluorescent moiety are linked to polyselena rings have been designed and prepared from 1,1′-bis(3-bromopropylseleno)ferrocene. Reaction of **L** with $[M(NCMe)_4](PF_6)_2$ (M = Pd and Pt) led to complexes $[ML](PF_6)_2$ (M = Pd and Pt). Crystal structure analysis revealed that after complexation, the macrocyclic ligand adopts the unusual *c*,*c*,*c* conformation due to intramolecular C−H···$\pi$ interactions from the hydrogen atoms of ferrocene moieties to the naphthalene ring. Electrochemical studies showed that in $[ML](PF_6)_2$ (M = Pd and Pt) the half-wave potential of the 1,1′-ferrocenediyl group shifts to much more positive potentials due to electron density withdrawn from Se donor atoms. Electrochemical and optical measurements were used to calculate HOMO and LUMO levels as well as HOMO−LUMO band gaps. Results were compared and correlated with the differences in molecular structures.

## INTRODUCTION

Design of functionalized receptors for development of potential chemosensors is an area of intense activity. In this context, of special interest is the design of multichannel-selective chemosensors, which can lead to acquisition of multiple signal expressions using single molecular entities. Toward this goal, the receptors can be built by combining chromogenic units, redox-active groups, or fluorescent signaling subunits near the binding sites. This is an unfamiliar area because relatively few examples describing coordination processes via multichannel signaling have been reported.[1] In addition, the mechanisms that regulate the interaction between probes and their targets are often poorly understood; hence, our ability to predict the structural requirements and design new probes is limited. In order to make perfect new receptor molecules, a better understanding of the relevant interaction mechanisms will be of significant help in a rational approach to such goals.

With these in mind, we are now undertaking a systematic study of macrocyclic fluorophore-containing polyselena[*n*]ferrocenophanes with the target to sense late transition metal ions. Systematic investigations have been reported on the synthesis, structure, and property of polythia[*n*]ferrocenophane by Sato and co-workers.[2] After complexation, the dative Fe−M bond was observed in some cases. In contrast, polyselena[*n*]ferrocenophanes have drawn less attention possibly due to the difficulty of their preparation.[2a] Our lab has embarked upon design of this class of ligands.[3] As a result of the macrocyclic effect, a suitable cavity size, and incorporation of soft donor Se atoms, they have proven to coordinate well to late transition metals. With incorporation of suitable signal units, they are also

**Received:** November 30, 2012
**Published:** April 30, 2013

   dx.doi.org/10.1021/ic302628y | *Inorg. Chem.* 2013, 52, 5786−5793

expected to be efficient electrochemical and optical sensors for late transition metal cations.

As a light-emitting fragment with strong emission and chemical stability, the naphthalene unit has been widely incorporated into chemosensors. From the viewpoint of synthesis, peri-substituted naphthalenes have attracted more and more attention due to the synthetic challenge and rigid $C_3$ chelating property.[4] The size and property of peri-atoms as well as the number and size of atoms attached to them are important. Heavier Group 16 (S, Se, Te) peri-substituted naphthalenes shed light on unknown reactivity and possibly development of a new concept of bonding.

In this paper, we presented the preparation, complexation, and characterization of three novel macrocyclic polyselena[$n$]-ferrocenophanes with a peri-substituted naphthalene unit. This study is expected to provide a useful design strategy for synthesis and application of multichannel sensors for late transition metal ions.

## EXPERIMENTAL SECTION

**Materials and General Procedures.** All reactions below were carried out under nitrogen using standard Schlenk techniques. All solvents were distilled from elemental alkali metal or Na/K alloy, except ethanol (which was degassed before use), acetonitrile, and dichloromethane (which were distilled over calcium hydride). $fcSe_3$ and $fc[Se(CH_2)_3Br]_2$ were prepared following the previously reported method.[3c,5]

**Physical Measurements.** Mass spectra were recorded using electron impact (EI) or positive-ion electrospray (ES): $m/z$ values have been rounded to the nearest integer or half-integer; assignments are based on isotopomers containing $^1H$, $^{12}C$, $^{56}Fe$, $^{80}Se$, and $^{106}Pd$ or $^{195}Pt$; expected isotope distribution patterns were observed. $^1H$ NMR spectra were measured in $CDCl_3$ at room temperature with a Varian Unity Plus 400 MHz NMR spectrometer. UV−vis absorption spectra were measured with a Varian UV−vis spectrophotometer. Fluorescence spectra were recorded at room temperature on a Horiba fluoromax-4 fluorescence spectrometer. For all measurements, excitation was at 287 nm. Both excitation and emission slit widths were 1.6 nm. Electrochemical measurements were performed at room temperature in a dry acetonitrile solution containing 0.1 M $[NBu_4][PF_6]$ electrolyte using an CHI 660C potentiostat system. The sweep rate for cyclic voltammetry was 100 mV $s^{-1}$. A three-electrode arrangement was used with a Pt working electrode, a Pt wire counter electrode, and a $Ag/Ag^+$ (0.01 M $AgNO_3$ in $CH_3CN$, referenced against ferrocene/ferrocenium) reference electrode. The sweep rate for cyclic voltammetry was 100 mV $s^{-1}$. A three-electrode arrangement was used with a Pt working electrode, a Pt wire counter electrode, and a $Ag/Ag^+$ (0.01 M $AgNO_3$ in $CH_3CN$, referenced against ferrocene/ferrocenium) reference electrode.

*Synthesis of* ***L1***. $NaBH_4$ (46 mg, 1.2 mmol) was added to an ethanol solution of 1,8-bis(selenocyanatomethyl)naphthalene (109 mg, 0.3 mmol) at 0 °C; the solution turned yellow in 5 min. Slowly warming to room temperature, the color disappeared quickly, accompanying intense $H_2$ gas evolution. $fc[Se(CH_2)_3Br]_2$ (176 mg, 0.3 mmol) in THF (5 mL) was then added slowly. The solution was left to stir at room temperature for 3 h. Solvent was removed by evaporation under reduced pressure. The residue was treated with water (25 mL) and then extracted with $CH_2Cl_2$ (3 × 25 mL). The extract was dried over $MgSO_4$, evaporated to dryness, and then subjected to column chromatography on $SiO_2$. Elution with hexane/dichloromethane (3:1) produced the target compound as a yellow solid. Yield: 35 mg (16%). $^1H$ NMR ($CDCl_3$): 7.76 ($C_{10}H_6$, d, 2H), 7.54 ($C_{10}H_6$, d, 2H), 7.38 ($C_{10}H_6$, s, 4H), 4.71 ($SeCH_2$, s, 4H), 4.29 ($C_5H_4$, m, 8H), 3.06 ($SeCH_2CH_2CH_2$, m, 8H), 2.25 ($SeCH_2CH_2CH_2$, m, 4H). ES MS: 738 ($[M]^+$).

*Synthesis of* ***L2***. $NaBH_4$ (46 mg, 1.2 mmol) was added to an ethanol solution of naphtho[1,8-*c*,*d*]-1,2-diselenole (86 mg, 0.3 mmol) at 0 °C; the solution turned purple in 5 min. Slowly warming to room temperature, the color turned to yellow green, accompanying intense $H_2$ gas evolution. Two hours later, $fc[Se(CH_2)_3Br]_2$ (195 mg, 0.3 mmol) in THF (10 mL) was then added slowly. The solution was left to stir at room temperature for 3 h. Solvent was removed by evaporation under reduced pressure. The residue was treated with water (25 mL) and then extracted with $CH_2Cl_2$ (3 × 25 mL). The extract was dried over $MgSO_4$, evaporated to dryness, and then subjected to column chromatography on $SiO_2$. Elution with hexane/dichloromethane (2:1) produced the target compound as an orange solid. Yield: 107 mg (50%). $^1H$ NMR ($CDCl_3$): 7.81 ($C_{10}H_6$, $H_{2+8}$, d, 2H), 7.74 ($C_{10}H_6$, $H_{4+6}$, d, 2H), 7.32 ($C_{10}H_6$, $H_{3+7}$, s, 4H), 4.22 ($C_5H_4$, m, 8H), 3.24 ($SeCH_2CH_2CH_2$, m, 8H), 2.21 ($SeCH_2CH_2CH_2$, m, 4H). ES MS: 710 ($[M]^+$).

*Synthesis of* ***L3***. **L3** was synthesized similar to **L2**, using naphtho[1,8-*c*,*d*]-1,2-dithiole instead of naphtho[1,8-*c*,*d*]-1,2-diselenole. The target compound is obtained as an orange solid with a yield of 60%. $^1H$ NMR ($CDCl_3$): 7.71 ($C_{10}H_6$, $H_{2+8}$, d, 2H), 7.60 ($C_{10}H_6$, $H_{4+6}$, d, 2H), 7.38 ($C_{10}H_6$, $H_{3+7}$, s, 4H), 4.91 ($C_5H_4$, m, 8H), 3.50, 3.23 ($CH_2CH_2CH_2$, m, 8H), 2.14 ($SCH_2CH_2CH_2$, m, 4H). ES MS: 618 ($[M]^+$).

*Synthesis of* ***1***. $PdCl_2$ (18 mg, 0.1 mmol) was refluxed in MeCN (30 mL) for 2 h to give a yellow solution of $[PdCl_2(NCMe)_2]$. After cooling, $AgPF_6$ (51 mg, 0.2 mmol) was added and stirring continued for another 15 min. **L1** (74 mg, 0.1 mmol) in $CH_2Cl_2$ (5 mL) was then added, and the mixture was stirred at room temperature for 24 h to give a blue liquid and a fine white precipitate of AgCl. The mixture was centrifuged to remove AgCl and reduced to 2 mL in vacuo. Diethyl ether (10 mL) was added to precipitate the product as a blue powder. Yield: 41 mg (48%). ES MS: 990.6 ($[M - PF_6]^+$).

*Synthesis of* ***2***−***6***. Synthesis was similar to **1**. **2**: brown powder. ES MS: 1072.3 ($[M - PF_6]^+$). **3**: brown black powder. ES MS: 964.4 ($[M - PF_6]^+$). **4**: brown powder. ES MS: 1050.7 ($[M - PF_6]^+$). **5**: black powder. ES MS: 866.7 ($[M - PF_6]^+$), 362.3 ($[M - 2PF_6]^{2+}$). **6**: brown powder. ES MS: 956.7 ($[M - PF_6]^+$), 406.3 ($[M - 2PF_6]^{2+}$).

**X-ray Data Collection and Structure Determinations.** Structural determinations were performed on a Bruker SMART APEX II CCD diffractometer using graphite-monochromatized Mo K$\alpha$ radiation ($\lambda$ = 0.71073 Å) at room temperature. A hemisphere of data was collected using a narrow-frame method with scan widths of 0.30° in $\omega$ and an exposure time of 10 s/frame. Data were integrated using the Siemens SAINT program,[6] with intensities corrected for Lorentz factor, polarization, air absorption, and absorption due to variation in the path length through the detector faceplate. Multiscan absorption corrections were applied. Structures were solved by direct methods and refined on $F^2$ by full-matrix least-squares using SHELXTL.[7] All non-hydrogen atoms were located from the Fourier maps and refined anisotropically. All H atoms were refined isotropically, with the isotropic vibration parameters related to the non-H atom to which they are bonded. Relevant details for structure refinements of **L1**−**L3**, **1**·$CH_3CN$·$H_2O$, **3**, **5**, and **6** are listed in Tables 1 and 2. Selected bond lengths and angles are given in the Supporting Information (Tables S1 and S2). CCDC 910592−910598 contain supplementary crystallographic data for this paper. These data can be obtained free of charge from the Cambridge Crystallographic Data Centre via www.ccdc.cam.ac.uk/data_request/cif.

**Theoretical Calculations.** All density functional theory (DFT) calculations were performed with the Gaussian 09 program package.[8] Geometrical structures of **L1**, **L2**, and **1**−**4** were fully optimized using the 6-31+G(d,p) basis set for nonmetal atoms (except for Se) and LanL2DZ basis set for metal and Se atoms. All structures were characterized as local minima by vibrational frequency analyses. Vertical excitation energies were obtained by time-dependent density functional theory (TDDFT) at the same level as geometry optimizations. The 6-31+G(d,p) rather than LanL2DZ basis set was used for Pd and Se atoms in TDDFT calculations of **L3**, **5**, and **6** to get the converged results. Natural bond orbital (NBO) calculations were performed to estimate the interaction energy between the orbitals.


dx.doi.org/10.1021/ic302628y | Inorg. Chem. 2013, 52, 5786−5793

**Table 1. Crystal Data and Structure Refinement Details of L1−L3**

| | L1 | L2 | L3 |
|---|---|---|---|
| formula | $C_{28}H_{30}FeSe_4$ | $C_{26}H_{26}FeSe_4$ | $C_{26}H_{26}FeS_2Se_2$ |
| fw | 738.21 | 710.16 | 616.36 |
| temp (K) | 293(2) | 293(2) | 296(2) |
| cryst size ($mm^3$) | 0.80 × 0.80 × 0.40 | 0.70 × 0.60 × 0.30 | 0.30 × 0.20 × 0.15 |
| cryst syst | triclinic | orthorhombic | orthorhombic |
| space group | *P*-1 | $P2_12_12_1$ | *Pbca* |
| *a*/*b*/*c* (Å) | 9.099(2)/ 10.769(3)/ 14.734(4) | 10.544(2)/ 14.235(2)/ 31.750(5) | 19.22(1)/ 11.52(1)/ 21.88(1) |
| $\alpha/\beta/\gamma$ (deg) | 73.561(4)/ 77.913(4)/ 70.602(5) | 90/90/90 | 90/90/90 |
| *V* ($Å^3$) | 1295.4(6) | 4766(1) | 4846(5) |
| *Z* | 2 | 8 | 8 |
| $D_{calcd}$ (Mg $m^{-3}$) | 1.893 | 1.980 | 1.690 |
| *F*(000) | 720 | 2752 | 2464 |
| $\mu$ ($mm^{-1}$) | 6.217 | 6.756 | 3.812 |
| $\theta$ range (deg) | 2.06−25.00 | 1.92−27.10 | 1.86−25.00 |
| *h*/*k*/*l* | −10, 6/−12,12/ −17,14 | −13, 12/−10,18/ −40,40 | −22,22/− 12,13/−25,26 |
| no. of reflns collected | 6494 | 27 730 | 32 329 |
| no. of indep reflns [$R_{int}$] | 4502 [0.0245] | 10 496 [0.0601] | 4265 [0.0571] |
| no. of obsd reflns [$I > 2\sigma(I)$] | 3586 | 7894 | 3298 |
| data/restraints/ params | 4502/0/314 | 10496/7/578 | 4265/0/280 |
| GOF | 1.084 | 1.016 | 1.088 |
| R1, wR2 indices [$I > 2\sigma(I)$] | 0.0268, 0.0537 | 0.0407, 0.0717 | 0.0294, 0.0625 |
| R1, wR2 indices (all data) | 0.0354, 0.0547 | 0.0656, 0.0762 | 0.0471, 0.0663 |
| largest diff. peak and hole ($eÅ^{-3}$) | 0.323, −0.470 | 1.005, −0.673 | 0.273, −0.402 |

## RESULTS AND DISCUSSION

**Synthesis.** **L1**−**L3** were synthesized in a stepwise manner, as shown in Scheme 1. For **L1**, reduction of 1,8-bis(selenocyanatomethyl)naphthalene with $NaBH_4$ afforded relative dianion, which was then reacted with 1,1′-bis(3-bromopropylseleno)ferrocene, $fc[Se(CH_2)_3Br]_2$ (fc = $[Fe(\eta^5\text{-}C_5H_4)_2]$), to give the target compound via [1 + 1] cyclization. **L2** and **L3** were obtained using naphtho[1,8-*c*,*d*]-1,2-diselenole or naphtho[1,8-*c*,*d*]-1,2-dithiole instead of 1,8-bis(selenocyanatomethyl)naphthalene.

Addition of 1 equiv of **L** in $CH_2Cl_2$ to a solution of $[M(NCMe)_4](PF_6)_2$ in acetonitrile at room temperature gave a dark blue (M = Pd) or red (M = Pt) liquid, from which $[ML](PF_6)_2$ could be precipitated by addition of diethyl ether (**1** M = Pd, **L** = **L1**; **2** M = Pt, **L** = **L1**; **3** M = Pd, **L** = **L2**; **4** M = Pt, **L** = **L2**; **5** M = Pd, **L** = **L3**; **6** M = Pt, **L** = **L3**). $^1H$ NMR spectra of **L** reveal the expected resonances. Mass spectra of **L** and complexes exhibit the correct isotopic patterns for the proposed formulas.

**Crystallographic Study.** Single crystals of **L1**−**L3** suitable for X-ray diffraction study were obtained as orange plates from $CH_2Cl_2$/hexanes. Crystals suitable for single-crystal X-ray analyses of the four complexes, **1**·$CH_3CN$·$H_2O$, **3**, **5**, and **6**, were obtained by slow diffusion of $Et_2O$ into a solution in MeCN. Structures are shown in Figure 1.

As rigid $C_3$ ligands, naphthalene imposes strain on non-hydrogen peri-atoms, which forces the two peri-atoms to form sub van der Waals contacts. Strain can also make nonbonded peri-substituted systems to distort from the idealized geometry in the naphthalene either by splaying, i.e., C−C−E angles varying from 120°, or by the naphthalene backbone becoming nonplanar.[9] Structures of **L1**−**L3** all obey this rule; the atoms attached on the naphthalene unit are displaced above and below the planes of the naphthalene backbones; this deviation decreases in the sequence Se > S > C.

In **L1**, the ferrocene unit adopts a "synclinal eclipsed"[10] conformation with a torsion angle C1−X1−X2−C6 of 69.3(2)° (X1 and X2 are the centroids of the two Cp rings). The nearest neighboring asymmetric units are connected to each other to form a dimer through intermolecular C−H···Se hydrogen bonds and the C−H···$\pi$ interactions from the hydrogen atoms of ferrocene moieties to the naphthalene rings. These dimers further interact along the *a* axis to form a one-dimensional chain by weak hydrogen bonds (see Figure S1, Supporting Information).

The asymmetric unit of **L2** comprises two molecules with different configurations. One ferrocene unit adopts a "synclinal eclipsed" conformation with a torsion angle C31−X1−X2−C36 of 61.0(4)°, and atoms C24 and C25 in one trimethylene chain are highly disordered with an occupancy of 0.60. Another adopts "synperiplanar" conformation with a torsion angle C1−X1−X2−C6 of 2.0(3)°, along with intramolecular C−H···$\pi$ interactions from the hydrogen atoms of ferrocene moieties to the naphthalene ring. In both configurations peri-selenium distances (3.162 or 3.147 Å) are comparable with those in analogous cyclic tetraselenide 8,9,19,20-tetrahydrodinaphtho-[1′,8′-*jk*:1,8-*bc*][1,5,9,13]tetraselenacyclohexadecine (3.167, 3.194 Å).[3a]

In **L3**, the ferrocene unit adopts a "synperiplanar" conformation with a torsion angle C1−X1−X2−C6 of 3.1(2)°. The nonbonded S···S distance is 3.066 Å, shorter than that in [1,8-*b*,*c*]-1,5-dithiocin (3.227(1) Å).[11]

On the other hand, the intramolecular Se1···Se2 distance (attached on Cp ring) (**L1**, 4.846 Å; **L2**, 3.855 and 4.562 Å; **L3**, 3.636 Å) is much shorter than that (5.200(2) Å) in $fcSe_4$.[3a]

After complexation, the metal atom is coordinated by the macrocyclic ligand in a slightly distorted square planar geometry and deviates from the best plane through four donor atoms by 0.21 (**1**·$CH_3CN$·$H_2O$) and 0.01 Å (**3**, **5**, **6**). In the solid state structures of these complexes the macrocyclic ligand adopts the *c*,*c*,*c* conformation.[12] Two trimethylene-chelate six-membered rings have the chair conformation. The same macrocyclic stereochemistry was observed in the solid state structure of $[M(\{16\}aneSe_4)](BF_4)_2$ (M = Pd or Pt),[13] whereas the *c*,*t*,*c* conformation was found for $[M(\{16\}aneSe_4)](PF_6)_2$·2MeCN and $[M(fcSe_4)](PF_6)_2$ (M = Pd or Pt).[14,3a] The present *c*,*c*,*c* arrangements can be attributed to intramolecular C−H···$\pi$ interactions from the hydrogen atoms of ferrocene moieties to the naphthalene ring. D···A distances of C−H···$\pi$ bonds range from 3.74 to 4.36 Å (Figure 1 and Table 3). The dihedral angle between the two planes (best plane through four donor atoms and the naphthalene ring) is 60.4°, 72.3°, 68.7°, and 68.9° for **1**·$CH_3CN$·$H_2O$, **3**, **5**, and **6**, respectively.

In each complex, the Se(S)−M−Se(S) (M = Pd and Pt) angles formed by the ferrocene and naphthalene unit are smaller than those formed by the trimethylene chains. Possibly, geometric requirements for optimization of the overlap between the Se(S) lone pairs and M orbitals play an important


dx.doi.org/10.1021/ic302628y | Inorg. Chem. 2013, 52, 5786−5793

**Table 2. Crystal Data and Structure Refinement Details of 1, 3, 5, and 6**

| | 1·$CH_3CN·H_2O$ | 3 | 5 | 6 |
|---|---|---|---|---|
| formula | $C_{30}H_{35}F_{12}FeNOP_2PdSe_4$ | $C_{26}H_{26}F_{12}FeP_2PdSe_4$ | $C_{26}H_{26}F_{12}FeP_2PdS_2Se_2$ | $C_{26}H_{26}F_{12}FeP_2PtS_2Se_2$ |
| fw | 1193.62 | 1106.50 | 1012.70 | 1101.39 |
| temp (K) | 293(2) | 293(2) | 296(2) | 296(2) |
| cryst size ($mm^3$) | 0.5 × 0.5 × 0.5 | 0.20 × 0.10 × 0.10 | 0.10 × 0.08 × 0.07 | 0.20 × 0.15 × 0.10 |
| cryst syst | triclinic | triclinic | triclinic | triclinic |
| space group | *P*-1 | *P*-1 | *P*-1 | *P*-1 |
| $a/b/c$ (Å) | 11.855(1)/13.128(1)/ 13.184(1) | 10.676(2)/11.868(2)/ 13.387(2) | 10.529(4)/11.795(4)/ 13.352(5) | 10.549(7)/11.809(8)/ 13.322(9) |
| $\alpha/\beta/\gamma$ (deg) | 84.566(2)/67.686(2)/ 80.060(2) | 75.271(3)/78.638(3)/ 83.311(3) | 75.373(4)/78.897(4)/ 83.309(4) | 75.320(8)/78.846(8)/ 82.675(8) |
| $V$ ($Å^3$) | 1868.7(3) | 1604.4(5) | 1570.5(10) | 1569.5(19) |
| $Z$ | 2 | 2 | 2 | 2 |
| $D_{calcd}$ (Mg $m^{-3}$) | 2.121 | 2.290 | 2.142 | 2.330 |
| $F(000)$ | 1152 | 1056 | 984 | 1048 |
| $\mu$ ($mm^{-1}$) | 4.939 | 5.740 | 3.679 | 7.560 |
| $\theta$ range (deg) | 2.26−25.00 | 1.95−25.00 | 1.60−25.00 | 1.60−25.00 |
| $h/k/l$ | −8, 14/−15,15/−11,15 | −12, 12/−14,13/−12,15 | −12,11/−13,13/−15,15 | −12,12/−13,14/−15,15 |
| no. of reflns collected | 9383 | 7926 | 11 206 | 10 846 |
| no. of indep reflns [$R_{int}$] | 6477 [0.0352] | 5549 [0.0234] | 5463 [0.0268] | 5439 [0.0303] |
| no. of obsd reflns [$I > 2\sigma(I)$] | 5099 | 4615 | 4439 | 4295 |
| data/restraints/params | 6477/0/469 | 5549/0/415 | 5463/0/415 | 5439/0/415 |
| GOF | 1.042 | 1.003 | 1.082 | 1.018 |
| R1, wR2 indices [$I > 2\sigma(I)$] | 0.0391, 0.0992 | 0.0552, 0.1664 | 0.0384, 0.1094 | 0.0364, 0.0970 |
| R1, wR2 indices (all data) | 0.0490, 0.1018 | 0.0647, 0.1743 | 0.0491, 0.1149 | 0.0525, 0.1027 |
| largest diff. peak and hole ($eÅ^{-3}$) | 1.214, −0.595 | 2.008, −1.751 | 1.026, −0.703 | 1.257, −0.968 |

**Scheme 1. Synthetic Routes of L1−L3**

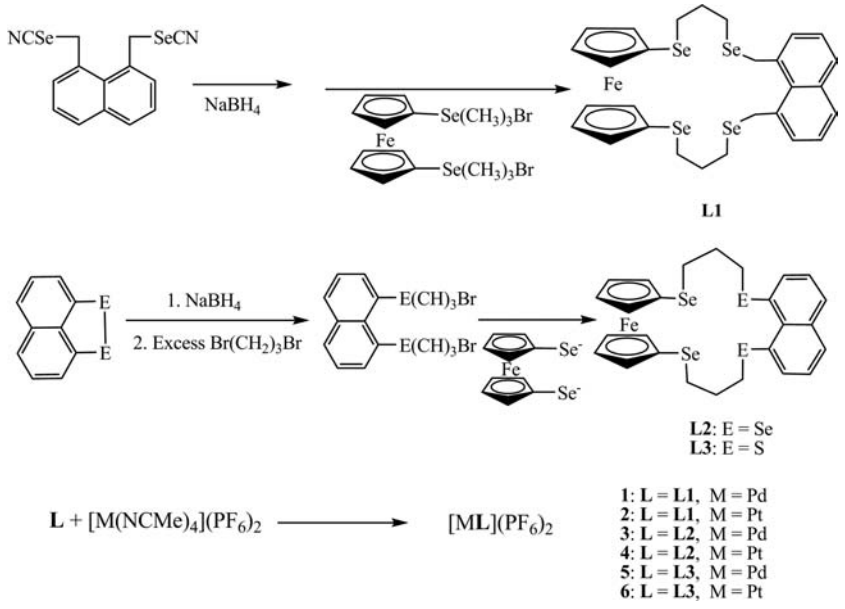


role here in addition to the major constraint posed by the dimension of the ferrocene and naphthalene unit.

After complexation, the ferrocene group in $[ML](PF_6)_2$ (M = Pd and Pt) adopts a "synperiplanar" conformation. The Fe···M distance is 4.073(1) Å for 1·$CH_3CN·H_2O$, 3.902(1) Å for **3**, 3.879(1) Å for **5**, and 3.887(2) Å for **6**. These distances are larger than the sum of the covalent radii of both metal atoms.

**Electrochemical Study.** The redox behavior was investigated by cyclic voltammetry (CV) in acetonitrile solution, and data obtained are summarized in Table 4.

The half-wave potentials for oxidation of the ferrocene moiety of **L** are all larger than that of $fcSe_4$ (32 mV), which mean it is more difficult to oxidize. Cyclic voltammograms of $[ML](PF_6)_2$ show one quasi-reversible redox wave from 642 to 784 mV in the potential range from −0.5 to +1.0 V. This is assigned to oxidation of the ferrocene moiety, as oxidation or reduction of the M(II) center occurs outside this potential range. There is a large positive potential shift in $E_{1/2}$ compared to the free ligand; $\Delta E$ is in the range from 580 to 716 mV (see Figure 2 and Figure S2, Supporting Information). Changing the metal from Pd to Pt did not bring about a significant change in


dx.doi.org/10.1021/ic302628y | Inorg. Chem. 2013, 52, 5786−5793

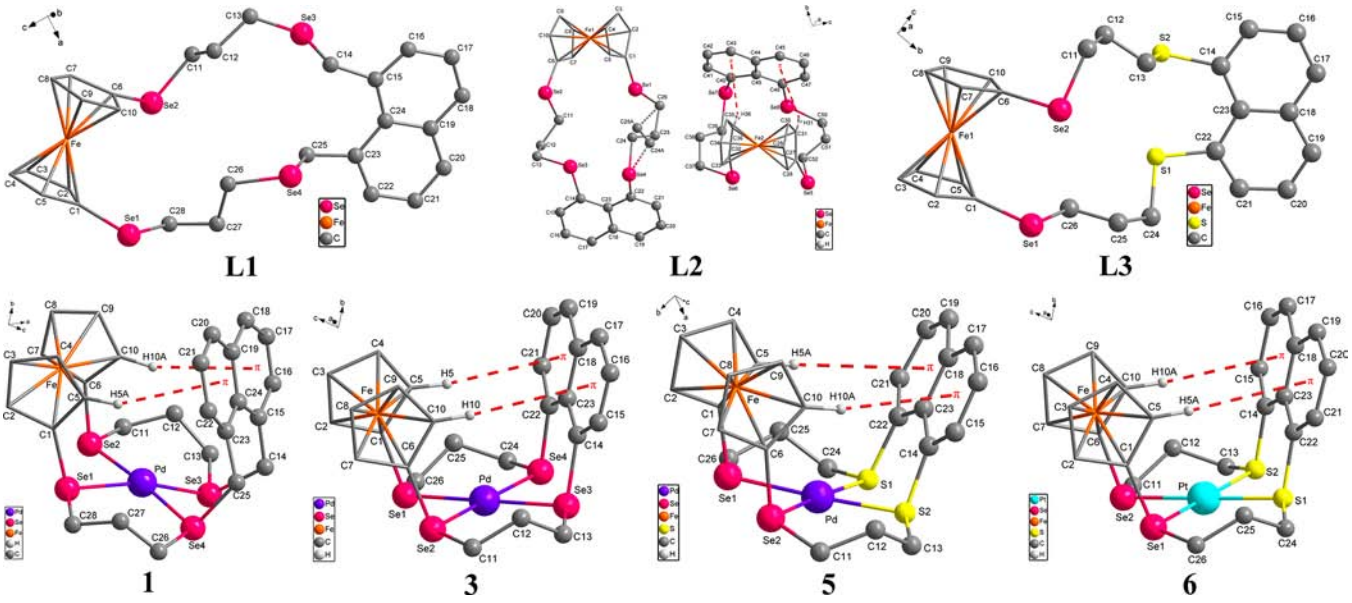


**Figure 1.** View of the structures with 30% probability ellipsoids. Less populated fraction of the disordered chain is shown with dashed bonds. Hydrogen atoms except hydrogen-bonding interactions are omitted for clarity.

**Table 3. Intramolecular Hydrogen-Bonding Interactions**[a]

| | D−H···A | $C_g$1 | $d$(D−H)/Å | $d$(H···A)/Å | $d$(D···A)/Å | ∠DHA/deg |
|---|---|---|---|---|---|---|
| **L2** | C31−H31···$C_g$1 | C44−C45−C46−C47−C48−C49 | 0.93 | 3.08 | 3.86 | 142.7 |
| | C36−H36···$C_g$1 | C40−C41−C42−C43−C44−C49 | 0.93 | 2.75 | 3.50 | 138.7 |
| **1** | C5−H5A···$C_g$1 | C19−C20−C21−C22−C23−C24 | 0.98 | 2.97 | 3.82 | 145.6 |
| | C10−H10···$C_g$1 | C15−C16−C17−C18−C19−C24 | 0.98 | 2.79 | 3.74 | 161.8 |
| **3** | C5−H5···$C_g$1 | C18−C19−C20−C21−C22−C23 | 0.98 | 3.09 | 4.05 | 169.0 |
| | C10−H10···$C_g$1 | C14−C15−C16−C17−C18−C23 | 0.98 | 3.38 | 4.36 | 171.7 |
| **5** | C5−H5A···$C_g$1 | C18−C19−C20−C21−C22−C23 | 0.98 | 3.35 | 4.32 | 170.9 |
| | C10−H10A···$C_g$1 | C14−C15−C16−C17−C18−C23 | 0.98 | 3.09 | 4.06 | 169.7 |
| **6** | C5−H5A···$C_g$1 | C18−C19−C20−C21−C22−C23 | 0.98 | 3.35 | 4.32 | 171.6 |
| | C10−H10A···$C_g$1 | C14−C15−C16−C17−C18−C23 | 0.98 | 3.11 | 4.09 | 171.7 |

[a] $C_g$1 is the centroid of the naphthalene unit.

**Table 4. Cyclic Voltammetric Data for L and Complexes**

| | M···Fe (Å) | $E_{1/2}$ ($\lvert E_{pa} - E_{pc}\rvert$) (mV)[a] | $\Delta E_{1/2}$ (mV) |
|---|---|---|---|
| **L1** | | 103 (171) | |
| **1** | 4.073(1) | 683 (113) | 580 |
| **2** | 4.251[b] | 696 (142) | 593 |
| **L2** | | 53 (98) | |
| **3** | 3.9013(3) | 642 (119) | 589 |
| **4** | 4.334[b] | 664 (257) | 611 |
| **L3** | | 68 (215) | |
| **5** | 3.879 (1) | 766 (124) | 698 |
| **6** | 3.887 (2) | 784 (174) | 716 |

[a] $E_{1/2}$ values are quoted relative to FcH /$[FcH]^+$. [b] Calculated at the PBE1PBE level.

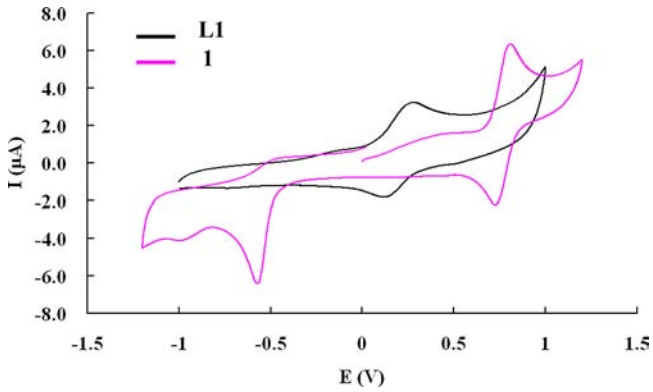


**Figure 2.** Cyclic voltammograms of **L1** and **1** in dry acetonitrile, 0.1 M $[NBu_4][PF_6]$, at a scan rate of 100 mV $s^{-1}$.

electrochemical behavior. Several literature works proved that the ferrocenyl group can act as a donor in the coordination sphere of the metal cation or behave as a moderately strong base toward the metal cation.[15] However, in current cases, the large Fe···M (Pd or Pt) distance (about 400 pm) gives a slim chance for direct interaction.

A previous study shows that selenoxide or sulfoxide formed on the electrochemical oxidation of Se (or S) peri-substituted naphthalenes. These phenomena were also observed in **L2** and **L3** (see Figures S3 and S4, Supporting Information), which can be attributed to removal of an electron from the occupied molecular orbitals, which is Se (or S) lone pair in character followed by attack by residue water in the acetonitrile solvent.[16]

**Computational Results.** To seek more detailed information on the electronic structures of the host−guest complexation, the geometries of **L1**, **L2**, and **1**−**4** were optimized by


dx.doi.org/10.1021/ic302628y | Inorg. Chem. 2013, 52, 5786−5793

DFT calculations (cf. Theoretical Calculations). Then, the electronic structural properties were evaluated using the same basis sets at the optimized geometries. Optimized geometries are in agreement with the above-mentioned experimental X-ray structures of **1** and **3**. Three kinds of functionals, B3LYP, B3PW91, and PBE1PBE, were used for absorption of **L1** (Figure 3). Among them, PBE1PBE results are in better agreement with experimental data than the others. PBE1PBE was then chosen to optimize geometries (Figure 4) and study the electronic structure properties described below (Figures 5−7). The conformational superpositions of the optimized and crystal structures of complexes **1** and **3** show a qualitative agreement between them.

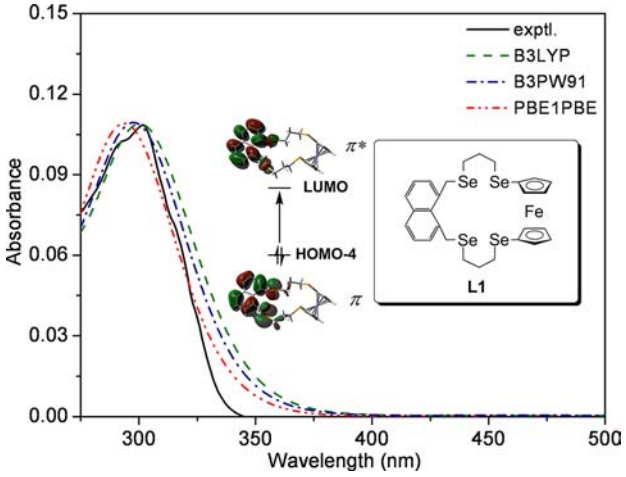


**Figure 3.** Absorption spectra and related molecular orbitals of **L1** obtained using different functionals.

TD-DFT calculation results show that, in free ligands, the maximum absorption wavelength corresponds to the transition between the $\pi$-type HOMO-4 and the $\pi^*$-type LUMO, mainly localized on the naphthalene unit (Figure 5). After complexation, the maximum absorption is dominated by the transition between the metal-centered d orbital and the naphthalene-centered $\pi^*$-type unoccupied molecular orbital, i.e., the metal-to-ligand charge transfer (MLCT).

The energy levels of the HOMO and LUMO orbitals are all upshifted with introduction of a metal atom to the ligands (Figure 6). Moreover, the energy level of the HOMO displays a significant exaltation by comparison to that of the LUMO. Consequently, the energy gap between the LUMO and the HOMO is markedly narrowed after complexation. It can be found from the natural bond orbital analysis that there is no evident interaction between the d orbitals of Fe and Pd atom (Table S4, Supporting Information). Occupation of each d orbital of Pd is close to 2, and the Fe−Pd interaction energy is close to zero, which is much less than that of Fe−C interaction (about 339 kcal/mol) in the ferrocene moiety. The negligible interaction between the Fe and the Pd atoms is consistent with the large Fe···Pd distance (about 400 pm) of them in the crystal structures. The remarkable perturbation of the redox wave of the ferrocene/ferrocenium redox couple can only be attributed to electron density withdrawn from the Se donor atoms after complexation.

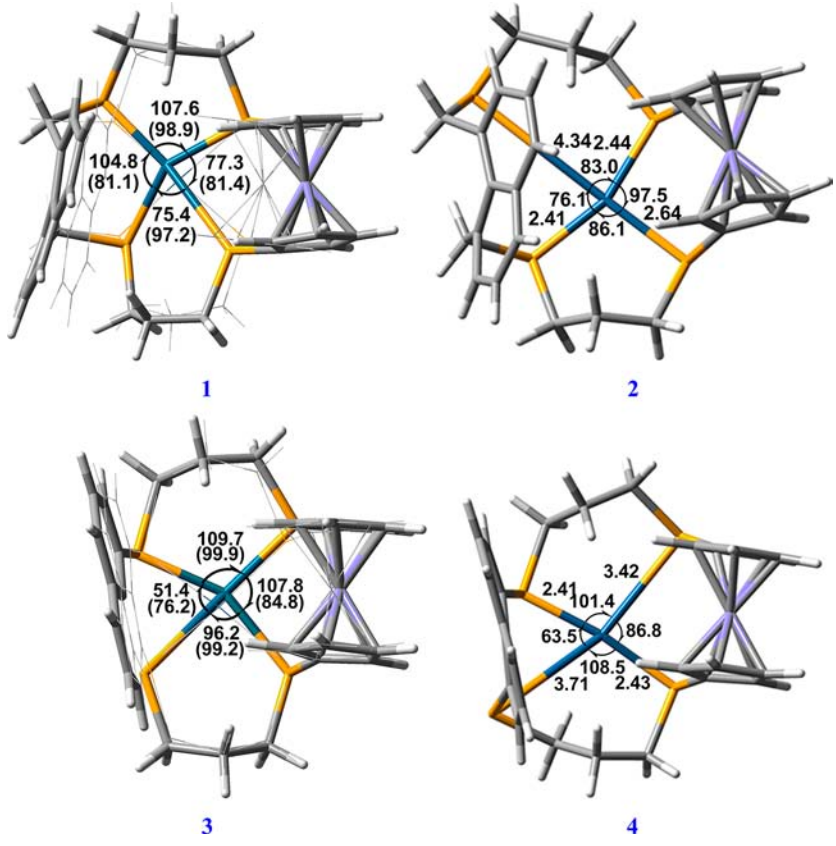


**Figure 4.** Optimized geometries of **1**−**4** at the PBE1PBE level (bond lengths are given in Angstroms and angles in degrees), and geometrical parameters of the X-ray structure (shown in thin lines) are given in parentheses for comparison.


dx.doi.org/10.1021/ic302628y | *Inorg. Chem.* 2013, 52, 5786−5793

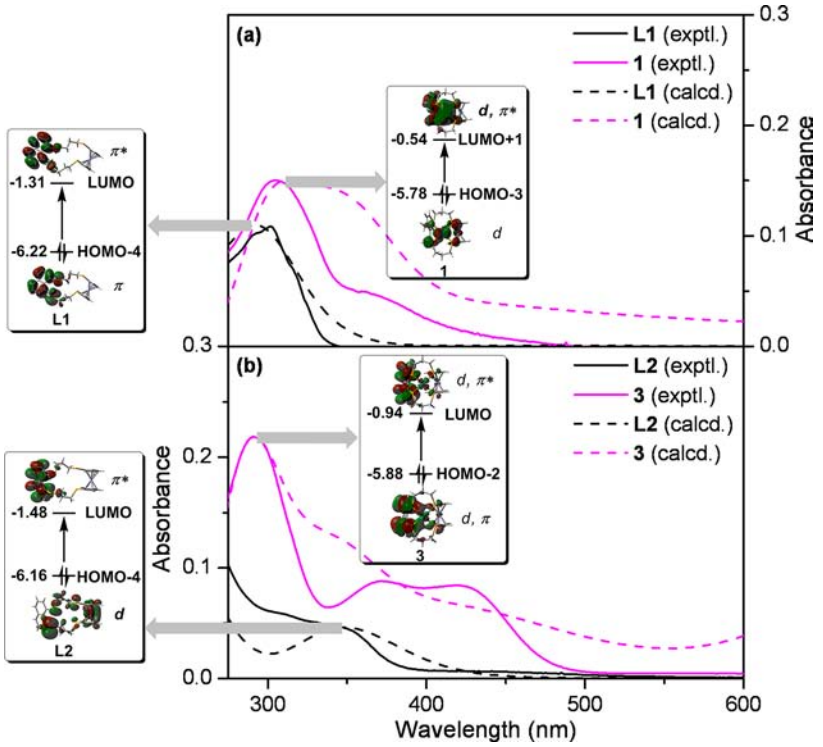


**Figure 5.** Absorption spectra and related molecular orbitals of metallocenes (**L1** and **L2**) and their Pd complexes (**1** and **3**) obtained from experiential observation and TD-DFT/PCM calculation.

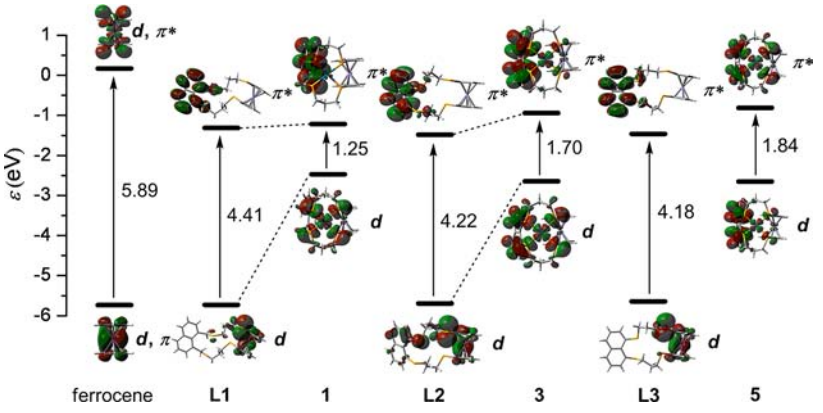


**Figure 6.** Energies of the HOMO and LUMO of various metallocenes calculated using the PBE1PBE functional (selection of basis sets for **L3** and **5** can be found in Theoretical Calculations).

The computed energy levels of the HOMO and LUMO as well as the HOMO−LUMO gap also agree well with those detected from cyclic voltammetry (Table S3, Supporting Information). The HOMO is determined according to the equation $E_{HOMO} = -(4.8 - E_{ref} + E_{ox,\ onset})$ eV, where $E_{ox,onset}$ is the potential at the onset of oxidation and $E_{ref}$ is the potential of the ferrocene reference.[17] The value of optical band gap is determined by the absorption onset obtained from the UV−vis absorption spectrum. The LUMO level is estimated by adding the optical band gap to the HOMO value. As shown in Figure 7, good agreement is found between the experimental observation and the theoretical investigation.

It should be mentioned that the study of the fluorescence behavior was carried out in acetonitrile solution. When excited at 287 nm, the ligands show typical structured naphthalene-like emission spectra at 329 nm (see Figure S6, Supporting Information). Complexes with $Pd^{2+}$ and $Pt^{2+}$ were not luminescent; the close proximity of the metal ions to the fluorophore provides pathways for energy- and electron-transfer processes, which cause fluorescence quenching.

## ■ CONCLUSIONS

This paper presents the synthesis and characterization of three novel macrocyclic polyselenaferrocenophanes containing a naphthalene unit and six Pd(II), Pt(II) complexes. X-ray crystallographic studies confirm that Pd(II) and Pt(II) ions are able to insert into the cavity of **L** to yield complexes with a square planar coordination geometry, with the ligand adopting a *c,c,c* configuration. Cyclic voltammetry shows that $E_{1/2}$ of the 1,1′-ferrocenediyl group shifts to more positive potentials in $[ML](PF_6)_2$ (M = Pd and Pt). The HOMO and LUMO levels were determined by experiments and theory calculations. Natural bond orbital analysis shows that there is no overlap between the d orbitals of Fe and the M atom. Consequently, no


dx.doi.org/10.1021/ic302628y | *Inorg. Chem.* 2013, 52, 5786−5793

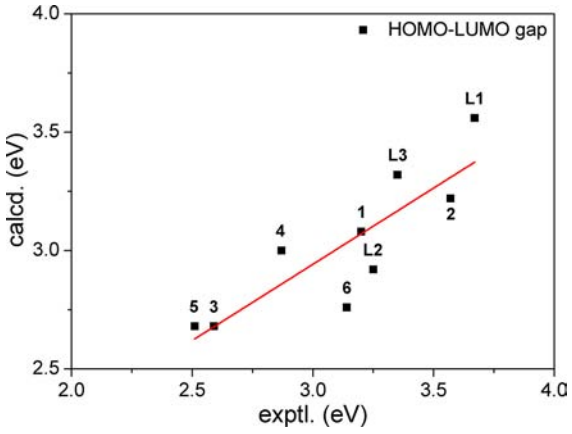


**Figure 7.** HOMO−LUMO gaps obtained by experiments and DFT calculations at the PBE1PBE level (selection of basis sets for **L3**, **5**, and **6** can be found in Theoretical Calculations).

direct Fe···Pd interaction exists in these complexes. We expect that our results and elaborations may provide a useful and pioneering guide to designing a new multichannel molecular sensor.

## ■ ASSOCIATED CONTENT

### Supporting Information

Experimental procedures, characterization data for synthesis, crystal data, calculated information, and X-ray structural data for CCDC 910592−910598 in CIF format. This material is available free of charge via the Internet at http://pubs.acs.org.

## ■ AUTHOR INFORMATION

### Corresponding Author

*Phone: +86-25-58139150 (S.J.); +86-25-83597408 (J.M.); +86-25-83587717 (D.Z.). Fax: +86-25-58139149 (S.J.); +86-25-83596131 (J.M.); +86-25-83172261 (D.Z.). E-mail: sjing@njut.edu.cn (S.J.); majing@mail.nju.edu.cn (J.M.); zhudr@njut.edu.cn (D.Z.).

### Notes

The authors declare no competing financial interest.

## ■ ACKNOWLEDGMENTS

We gratefully acknowledge financial support from the National Natural Science Foundation (Grant Nos. 21171092, 21171093, 20825312, and 21273102) and Foundation of State Key Laboratory of Materials-Oriented Chemical Engineering, NJUT (Grant No. KL12-06).

## ■ REFERENCES

(1) For example, see: (a) Sancenon, F.; Benito, A.; Hernández, F. J.; Lloris, J. M.; Martínez-Máñez, R.; Soto, J. *Eur. J. Inorg. Chem.* **2002**, 866. (b) Otón, F.; Tárraga, A.; Velasco, M. D.; Espinosa, A.; Molina, P. *Chem. Commun.* **2004**, 1658. (c) Otón, F.; Tárraga, A.; Espinosa, A.; Bautista, D.; Molina, P. *J. Org. Chem.* **2005**, *70*, 6603. (d) Otón, F.; Tárraga, A.; Espinosa, A.; Velasco, M. D.; Molina, P. *J. Org. Chem.* **2006**, *71*, 4590. (e) Otón, F.; Espinosa, A.; Tárraga, A.; de Arellano, C. R.; Molina, P. *Chem.—Eur. J.* **2007**, *13*, 5742. (f) Molina, P.; Tárraga, A.; Caballero, A. *Eur. J. Inorg. Chem.* **2008**, 3401. (g) Zapata, F.; Caballero, A.; Espinosa, A.; Tárraga, A.; Molina, P. *Inorg. Chem.* **2009**, *48*, 11566. (h) Alfonso, M.; Espinosa, A.; Tárraga, A.; Molina, P. *Org. Lett.* **2011**, *13*, 2078. (i) Zhang, B.; Xu, J.; Zhao, Y.; Duan, C.; Cao, X.; Meng, Q. *Dalton Trans.* **2006**, 1271.

(2) (a) In *Ferrocenes: Homogeneous catalysis-organic synthesis-materials science*; Togni, A., Hayashi, T., Eds.; VCH: Weinheim, Germany, 1995. (b) Sato, M.; Anano, H. *J. Organomet. Chem.* **1998**, *555*, 167. (c) Siemeling, U.; Auch, T. *Chem. Soc. Rev.* **2005**, *34*, 584.

(3) (a) Jing, S.; Morley, C. P.; Gu, C.; Vaira, M. D. *Dalton Trans.* **2010**, *39*, 8812. (b) Li, Z.; Jing, S.; Morley, C. P.; Gu, C. *Inorg. Chem. Commun.* **2009**, *12*, 440. (c) Jing, S.; Gu, C.; Ji, W.; Yang, B. *Inorg. Chem. Commun.* **2009**, *12*, 846. (d) Gu, C.; Jing, S.; Yang, B.; Wei, Y.; Zhang, W.; Ji, W. *Chin. Inorg. Chim. Acta* **2010**, *26*, 339. (e) Zhang, X.; Qin, Y.; Xiao, F.; Jing, S.; Ji, W. *Chin. Inorg. Chim. Acta* **2012**, *28*, 1015. (f) Gu, C.; Jing, S.; Ji, W.; Li, Z. *Inorg. Chim. Acta* **2010**, *363*, 1604.

(4) (a) Kilian, P.; Knight, F. R.; Woollins, J. D. *Chem.—Eur. J.* **2011**, *17*, 2302. (b) Kilian, P.; Knight, F. R.; Woollins, J. D. *Coord. Chem. Rev.* **2011**, *255*, 1387.

(5) Broussier, R.; Abdulla, A.; Gautheron, B. *J. Organomet. Chem.* **1987**, *332*, 165.

(6) *SAINT*; Siemens Analytical X-ray Instruments: Madison, WI, 1996.

(7) *SHELXTL Reference Manual*, version 5.0; Siemens Industrial Automation, Analytical Instruments: Madison, WI, 1997.

(8) Frisch, M. J.; Trucks, G. W.; Schlegel, H. B.; Scuseria, G. E.; Robb, M. A.; Cheeseman, J. R.; Scalmani, G.; Barone, V.; Mennucci, B.; Petersson, G. A.; Nakatsuji, H.; Caricato, M.; Li, X.; Hratchian, H. P.; Izmaylov, A. F.; Bloino, J.; Zheng, G.; Sonnenberg, J. L.; Hada, M.; Ehara, M.; Toyota, K.; Fukuda, R.; Hasegawa, J.; Ishida, M.; Nakajima, T.; Honda, Y.; Kitao, O.; Nakai, H.; Vreven, T.; Montgomery, Jr., J. A.; Peralta, J. E.; Ogliaro, F.; Bearpark, M.; Heyd, J. J.; Brothers, E.; Kudin, K. N.; Staroverov, V. N.; Kobayashi, R.; Normand, J.; Raghavachari, K.; Rendell, A.; Burant, J. C.; Iyengar, S. S.; Tomasi, J.; Cossi, M.; Rega, N.; Millam, N. J.; Klene, M.; Knox, J. E.; Cross, J. B.; Bakken, V.; Adamo, C.; Jaramillo, J.; Gomperts, R.; Stratmann, R. E.; Yazyev, O.; Austin, A. J.; Cammi, R.; Pomelli, C.; Ochterski, J. W.; Martin, R. L.; Morokuma, K.; Zakrzewski, V. G.; Voth, G. A.; Salvador, P.; Dannenberg, J. J.; Dapprich, S.; Daniels, A. D.; Farkas, Ö.; Foresman, J. B.; Ortiz, J. V.; Cioslowski, J.; Fox, D. J. *Gaussian 09*, revision A.02; Gaussian, Inc.: Wallingford, CT, 2009.

(9) Aucott, S. M.; Milton, H. L.; Robertson, S. D.; Slawin, A. M. Z.; Woollins, J. D. *Heteroatom Chem.* **2004**, *15*, 530.

(10) Fujihara, H.; Yabe, M.; Ilemori, N.; Furukawa, N. *J. Chem. Soc., Perkin Trans. 1* **1993**, 2145.

(11) Glass, R. S.; Andruski, S. W.; Broeker, J. L.; Firouzabadi, H.; Steffen, L. K.; Wilson, G. S. *J. Am. Chem. Soc.* **1989**, *111*, 4036.

(12) Panda, A. *Coord. Chem. Rev.* **2009**, *253*, 1056.

(13) Batchelor, R. J.; F. Einstein, W. B.; Gay, I. D.; Gu, J. H.; Pinto, B. M.; Zhou, X. *Inorg. Chem.* **1996**, *35*, 3667.

(14) Champness, N. R.; Kelly, P. F.; Levason, W.; Reid, G.; Slawin, A. M. Z.; Williams, D. *Inorg. Chem.* **1995**, *34*, 651.

(15) (a) Akabori, S.; Kumagai, T.; Shirahige, T.; Sato, S.; Kawazoe, K.; Tamura, C.; Sato, M. *Organometallics* **1987**, *6*, 2105. (b) Medina, J. C.; Goodnow, T. T.; Rojas, M. T.; Atwood, J. L.; Lynn, B. C.; Kaifer, A. E.; Gokel, G. W. *J. Am. Chem. Soc.* **1992**, *114*, 10583. (c) Otón, F.; Ratera, I.; Espinosa, A.; Wurtz, K.; Parella, T.; Tárraga, A.; Veciana, J.; Molina, P. *Chem.—Eur. J.* **2010**, *16*, 1532. (d) Caballero, A.; Tormos, R.; Espinosa, A.; Velasco, M. D.; Tárraga, A.; Miranda, M. A.; Molina, P. *Org. Lett.* **2004**, *6*, 4599.

(16) (a) Glass, R. S.; Andruski, S. W.; Broeker, J. L.; Firouzabadi, H.; Steffen, L. K.; Wilson, G. S. *J. Am. Chem. Soc.* **1989**, *111*, 4036. (b) Fujihara, H.; Yabe, M.; Ilemori, M.; Furukawa, N. *J. Chem. Soc. Perkin Trans. 1* **1993**, 2145. (c) Fujihara, H.; Yabe, M.; Furukawa, N. *J. Chem. Soc., Perkin Trans. 1* **1996**, 1783.

(17) (a) Al-Ibrahim, M.; Roth, H. K.; Zhokhavets, U.; Gobsch, G.; Sensfuss, S. *Sol. Energ. Mater. Sol. C* **2005**, *85*, 13. (b) Pommerehne, J.; Vestweber, H.; Guss, W.; Mahrt, R. F.; Porsch, M.; Daub, J. *Adv. Mater.* **1995**, *7*, 551.